

Electronic Supplementary Materials

## Shape Adaptation of Quinine in Cyclodextrin Cavities: NMR studies

Jacek Wójcik<sup>1</sup>, Andrzej Ejchart<sup>1</sup>, Michał Nowakowski<sup>2,\*</sup>

<sup>1</sup> Institute of Biochemistry and Biophysics, Polish Academy of Sciences, Pawinskiego 5A, 02-106 Warszawa, Poland; jacekw@ibb.waw.pl (J.W.); aejchart@ibb.waw.pl (A.E.)

<sup>2</sup> Faculty of Chemistry, Biological and Chemical Research Centre, University of Warsaw Zwirki i Wigury 101, 02-089 Warsaw, Poland

\* Correspondence: lyam@chem.uw.edu.pl

### Contents:

Materials and sample preparation

Detailed parameters NMR measurements

Figure S1. Dihedral angles which undergo conformational changes in quinine solution.

Figure S2. <sup>1</sup>H NMR spectrum (500 MHz) of quinine.

Table S1. <sup>1</sup>H chemical shifts of quinine in D<sub>2</sub>O.

Table S2. *J*<sub>H,H</sub> scalar couplings of quinine in D<sub>2</sub>O at pH 10.5.

Figure S3. Set of <sup>1</sup>H NMR titration spectra for Q/αCD complex at pH 10.5.

Figure S4. Set of <sup>1</sup>H NMR titration spectra for Q/βCD complex at pH 10.5.

Figure S5. Set of <sup>1</sup>H NMR titration spectra for Q/γCD complex at pH 10.5.

Table S3. Values of association constants, *K*<sub>a</sub>, determined for Q/CD complexes.

Table S4. *CIS* values for <sup>1</sup>H and <sup>13</sup>C resonances Q/CD complexes at pH 10.5 and 25°C.

Table S5. *CIS* values for <sup>1</sup>H and <sup>13</sup>C resonances Q/CD complexes at pH 7.3 and 25°C.

Figure S6. Stripe of 2D ROESY spectrum for Q/βCD complex.

Table S6. Some parameters for the 23 DFT derived lowest-energy conformations.

Figure S7. Histogram of dipole moments for the 23 lowest-energy conformations.

Figure S8. Correlations between DFT derived <sup>13</sup>C shielding constants and experimental chemical shifts for the proton bearing <sup>13</sup>C nuclei of quinine at pH 10.5.

DFT based parametrization of Karplus equation for vicinal <sup>3</sup>*J*<sub>2,9</sub> coupling constant in neutral quinine molecule in aqueous solution including Figure S9.

Influence of Q/CD complex formation on values of vicinal <sup>3</sup>*J*<sub>5,10</sub> coupling constant including Figure S10 and Table S7.

## Materials and sample preparation

Quinine was obtained from POCh (Gliwice, Poland).  $\alpha$ -,  $\beta$ - and  $\gamma$ -cyclodextrins from Sigma-Aldrich (St. Louis, MO) were used without further purification. The D<sub>2</sub>O from Armar Chemicals (Dottingen, Switzerland) contained 99.8% D. Quinine was dissolved in D<sub>2</sub>O to a concentration of ~0.5 mmol/L. Part of quinine solution was separated from the rest and cyclodextrin was added to it in large excess over quinine. These basic solutions, containing either quinine or quinine and cyclodextrin, were mixed afterwards together in order to prepare seven to twelve NMR samples (0.65 mL total volume) of various cyclodextrin/quinine molar ratios,  $R$ , so that the concentrations of quinine remained constant during the titrations. Cyclodextrin/quinine molar ratios were finally determined by <sup>1</sup>H signal integration of CD anomeric protons versus four protons of quinine (H3', H5', H7', H8'), rather than to weigh a cyclodextrin which can contain an imprecisely known amount of water, since CDs crystallize from water as hydrates of variable composition.<sup>3-6</sup> The maximum  $R$  values used in the titrations reached 39.6, 16.5, and 19.2 for Q/ $\alpha$ CD, Q/ $\beta$ CD, and Q/ $\gamma$ CD, respectively.

On the basis of the literature values of quinine pK<sub>a</sub> values<sup>7</sup> and titration curve the pH values for the complexation experiments have been chosen as 10.5, 7.3, and 2.5. These values correspond to the neutral, singly protonated, and double protonated molecule, respectively. In order to maintain constant pH value the following buffer solutions have been applied: the carbonate buffer - for pH 10.5, phosphatic buffer - for pH 7.3 and KCl/HCl buffer - for pH 2.5. The carbonate buffer was composed of Na<sub>2</sub>CO<sub>3</sub> and NaHCO<sub>3</sub> in 2 to 1 molar ratio. The phosphatic buffer was composed of Na<sub>2</sub>DPO<sub>4</sub> and NaD<sub>2</sub>PO<sub>4</sub> in 2 to 1 molar ratio. The KCl/HCl buffer was composed of KCl and DCl in 10 to 1 molar ratio. The pH was maintained in each case with 30 mM buffer concentration. All pH measurements were carried out in D<sub>2</sub>O solutions and all pH values are reported as isotope uncorrected pH meter readings.

## Detailed parameters NMR measurements

All titration measurements were performed at a magnetic field of 11.7 T, using a Varian (Palo Alto, CA) 500 MHz INOVA, spectrometer. NMR spectra were measured at a temperature carefully adjusted to 25°C with an accuracy of 0.1°C and was checked by an ethylene glycol reference sample.<sup>1</sup> All chemical shifts in <sup>1</sup>H NMR spectra are reported with respect to external DSS-d<sub>4</sub>. Chemical shifts of <sup>13</sup>C signals were referenced indirectly using the 0.251449530 frequency ratio <sup>13</sup>C/<sup>1</sup>H.<sup>2</sup>

<sup>1</sup>H chemical shifts were determined from 1D <sup>1</sup>H NMR spectra measured with 10.5 s relaxation delay followed by 1.5 s preirradiation of residual HDO resonance. A long repetition time allowed avoiding partial saturation of aromatic quinine protons displaying longitudinal relaxation times up to 3.0 s. Acquisition parameters were as follows: sweep width 4293 Hz, number of acquired points 21 k, and 512 scans. FIDs were processed with 0.1 Hz line broadening and zero-filled to 128 k, resulting in a 0.065 Hz spectrum digital resolution. The spectrum of quinine at pH 10.5 has been fully analyzed by means of the STSIT program (S. Szymanski, unpublished program) allowing the precise determination of all chemical shifts and <sup>1</sup>H-<sup>1</sup>H coupling constants. The STSIT program involves a nonlinear, least squares fit of the relevant spectral parameters to the experimental line shape. It is equivalent to the program DAVINS by Stephenson and Binsch distributed once by the Quantum Chemistry Programs Exchange.<sup>8,9</sup>

<sup>13</sup>C chemical shifts were obtained from 2D <sup>1</sup>H/<sup>13</sup>C HSQC spectra.<sup>10</sup> In the <sup>13</sup>C dimension a sweep width of 19 kHz and 512 complex data points, were used. Each of 128 scans was preceded by a 1 s relaxation delay. FIDs were multiplied by squared cosine weighting functions and zero-filled to 4 k in <sup>13</sup>C dimension. Digital resolution in the <sup>13</sup>C dimension was equal to 9.2 Hz.

Acquisition parameters of ROESY spectra<sup>11</sup> were set to the following parameters: sweep width 4293 Hz, acquired data points in directly and indirectly

detected dimensions were 676 and 256, respectively. Each of 96 scans was preceded by a 1.0 s relaxation delay and mixing time was set to 500 ms. FIDs were multiplied by squared cosine weighting functions. In both dimensions zero-filling to 2 k was applied.

## References

- 1 D. S. Raiford, C. L. Fisk, E. D. Becker, *Anal. Chem.*, 1979, **51**, 2050-2051.
- 2 D. S. Wishart, C. G. Bigam, C. G. Yao, F. Abildgaard, H. J. Dyson, E. Oldfield, J. L. Markley and B. D. Sykes, *J. Biomol. NMR*, 1995, **6**, 135-140.
- 3 W. Saenger, J. Jacob, K. Gessler, T. Steiner, D. Hoffmann, H. Sanbe, K. Koizumi, S. M. Smith and T Takaha, *Chem. Rev.*, 1998, **98**, 1787-1802.
- 4 F. W. Lichtenthaler, S. Immel, *Liebigs Ann.*, 1996, 27-37.
- 5 K. A. Connors, *Chem. Rev.*, 1997, **97**, 1325-1357.
- 6 Z. Dang, L. X. Song, X. Q. Guo F. Y. Du, J. Yang, J. Yang, *Curr. Org. Chem.*, **15**, 848-861.
- 7 J. L. Irvin and E. M. Irvin, *J. Biol. Chem.*, 1948, **174**, 577-587.
- 8 D. S. Stephenson and G. Binsch, *J. Magn. Reson.*, 1980, **37**, 395-407.
- 9 D. S. Stephenson and G. Binsch, *J. Magn. Reson.*, 1980, **37**, 409-430.
- 10 G. Bodenhausen and D. J. Ruben, *Chem. Phys. Lett.*, 1980, **69**, 185-189.
- 11 A. Bax and D. G. Davis, *J. Magn. Reson.*, 1985, **63**, 207-213.

## Figure S1

Definitions of the dihedral angles which undergo conformational changes in quinine solution. H<sub>2</sub>-C<sub>2</sub>-C<sub>9</sub>-H<sub>9</sub>: in figure  $\phi_1 = +60$  deg; H<sub>9</sub>-C<sub>9</sub>-C<sub>4'</sub>-C<sub>3'</sub>: in figure  $\phi_2 = +90$  deg; H<sub>5</sub>-C<sub>5</sub>-C<sub>10</sub>-H<sub>10</sub>: in figure  $\phi_3 = +90$  deg; C<sub>5'</sub>-C<sub>6</sub>-O-C<sub>Me</sub>: in figure  $\phi_4 = +90$  deg, H-O-C<sub>9</sub>-H<sub>9</sub>: in figure  $\phi_5 = +60$  deg.

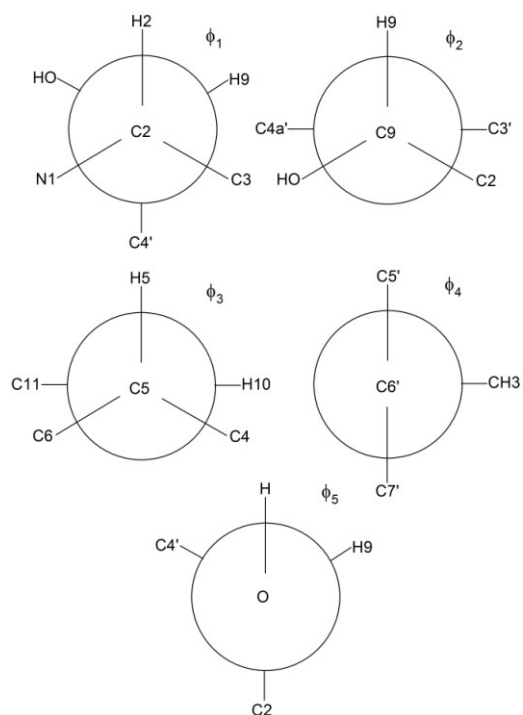


**Figure S2**

$^1\text{H}$  NMR spectrum (500 MHz) of quinine in  $\text{D}_2\text{O}$  ( $c=0.53$  mmol/L) at pH 10.5 and  $t=25^\circ\text{C}$ . Singlet resonance of methoxy group at 3.992 ppm is not show.

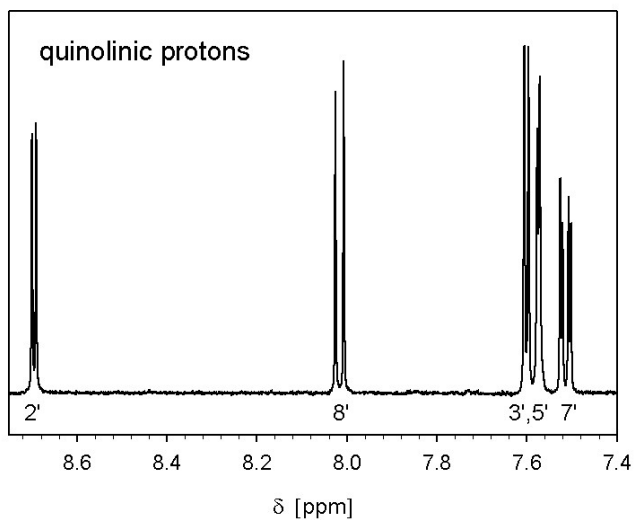
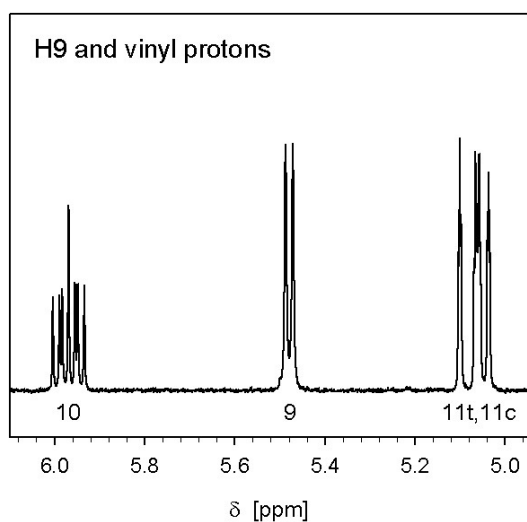
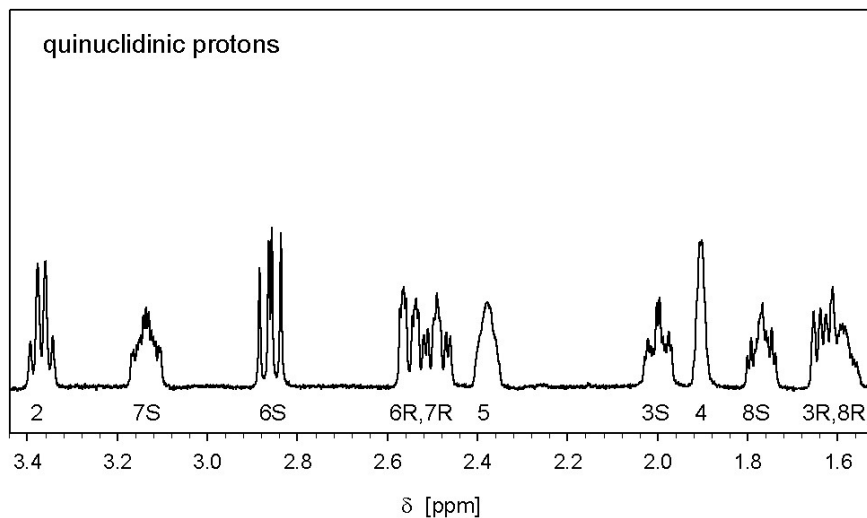


**Table S1**

<sup>1</sup>H (part A) and <sup>13</sup>C (part B) chemical shifts of quinine resonances in D<sub>2</sub>O (c≈0.5 mmol/L) at 25°C. Chemical shifts of quaternary <sup>13</sup>C nuclei have been not determined.

Part A	pH 10.5	pH 7.3	pH 2.5
Quinoline moiety			
H2'	8.695	8.745	8.951
H3'	7.600	7.723	8.276
H5'	7.573	7.446	7.599
H7'	7.513	7.560	7.857
H8'	8.016	8.053	8.225
Me	3.992	4.006	4.076
Linker			
H9	5.480	5.934	6.185
Quinuclidine moiety			
H2	3.369	3.724	3.703
H3R	1.637	2.074	2.163
H3S	2.000	1.820	1.660
H4	1.905	2.198	2.215
H5	2.378	2.834	2.870
H6R	2.550	3.248	3.308
H6S	2.861	3.524	3.633
H7R	2.491	3.226	3.320
H7S	3.137	3.970	4.172
H8R	1.588	1.953	1.980
H8S	1.771	2.115	2.170
H10	5.969	5.789	5.732
H11c	5.048	5.081	5.057
H11t	5.084	5.126	5.113
Part B	pH 10.5	pH 7.3	pH 2.5
Quinoline moiety			
C2'	150.39	150.33	143.08
C3'	122.58	122.33	122.44
C5'	105.07	104.64	104.75
C7'	124.64	124.83	129.81
C8'	132.88	133.23	125.83
Me	58.73	58.79	59.05
Linker			
C9	74.69	71.03	70.26
Quinuclidine moiety			
C2	63.33	62.72	62.15
C3	27.31	22.53	21.02
C4	29.89	28.72	28.54
C5	41.22	39.19	38.86
C6	57.70	56.95	53.99
C7	44.31	46.557	46.96
C8	29.37	26.36	26.03
C10	145.24	140.90	ND
C11	116.92	118.84	118.90

**Table S2**

$J_{H,H}$  scalar couplings of quinine in D<sub>2</sub>O at pH 10.5. The STSIT, unpublished FORTRAN program by S. Szymanski, was used to fit spectral parameters to the experimental line shape with the estimated accuracy better 0.1 Hz for scalar coupling constants. Longitudinal relaxation times  $T_1$  were estimated with inversion-recovery sequence with the accuracy of ca. 0.1 s.

	$^2J$ (Hz)	$^3J$ (Hz)	$^4J$ (Hz)	$^5J$ (Hz)	$T_1$ (s)
H2'		$J_{2,3'}=4.7$			2.4
H3'					1.3
H5'			$J_{5,7'}=2.7$		2.0
H7'		$J_{7,8'}=9.3$			0.8
H8'					2.7
Me					1.0
H9		$J_{2,9}=8.1$			<sup>a</sup>
H2		$J_{2,3R}=7.3$ $J_{2,3S}=9.6$			<sup>a</sup>
H3R	$J_{3R,3S}=13.7$	$J_{3R,4}=7.4$			<sup>a</sup>
H3S		$J_{3S,4}=4.2$	$J_{3S,5}=2.7$		<sup>a</sup>
H4		$J_{4,5}=1.0$ $J_{4,8R}=5.8$ $J_{4,8S}=3.7$	$J_{4,7R}=1.3$ $J_{4,7S}=2.5$	$J_{4,11c}=0.4$ $J_{4,11t}=0.2$	<sup>a</sup>
H5		$J_{5,10}=7.4$ $J_{5,11c}=1.7$ $J_{5,11t}=1.7$			<sup>a</sup>
H6R	$J_{6R,6S}=13.7$	$J_{5,6R}=4.5$	$J_{4,6R}=0.9$ $J_{6R,10}=2.5$		<sup>a</sup>
H6S		$J_{5,6S}=10.1$	$J_{4,6S}=0.7$ $J_{6S,10}=0.4$		<sup>a</sup>
H7R	$J_{7R,7S}=13.8$	$J_{7R,8R}=11.0$ $J_{7R,8S}=4.6$			<sup>a</sup>
H7S		$J_{7S,8R}=5.9$ $J_{7S,8S}=10.5$			<sup>a</sup>
H8R	$J_{8R,8S}=12.6$				<sup>a</sup>
H8S					<sup>a</sup>
H10		$J_{10,11c}=10.4$ $J_{10,11t}=17.3$	$J_{4,10}=0.4$		1.6
H11c	$J_{11c,11t}=1.3$				1.3
H11t					1.4

<sup>a</sup> rough estimation of  $T_1$  for aliphatic  $^1H$  resonances:  $0.4 \text{ s} < T_1 < 0.9 \text{ s}$

**Figure S3**

Set of  $^1\text{H}$  NMR titration spectra for Q/ $\alpha$ CD complex at pH 10.5. Right part – quinuclidine protons, left part – quinoline protons.

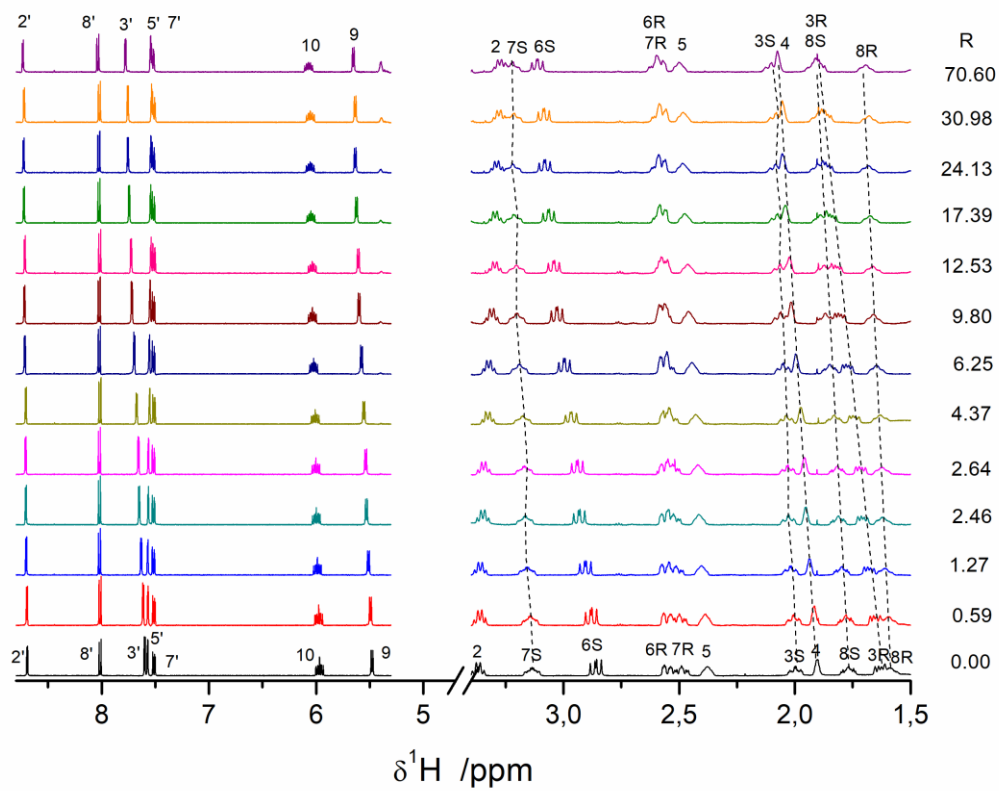


**Figure S4**

Set of  $^1\text{H}$  NMR titration spectra for Q/ $\beta$ CD complex at pH 10.5. Upper part – quinuclidine protons, lower part – quinoline protons.

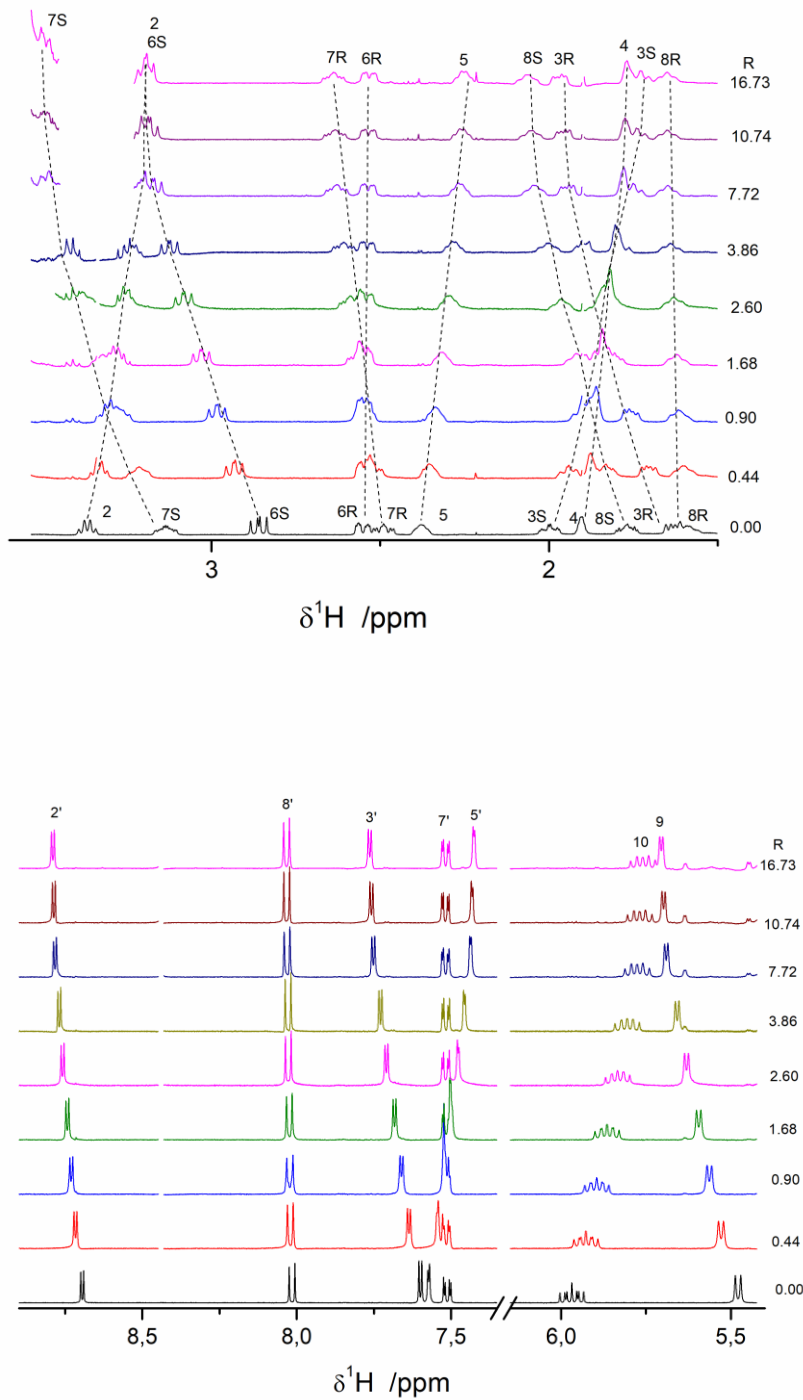




**Figure S5**

Set of  $^1\text{H}$  NMR titration spectra for Q/ $\gamma$ CD complex at pH 10.5. Right part – quinuclidine protons, left part – quinoline protons.

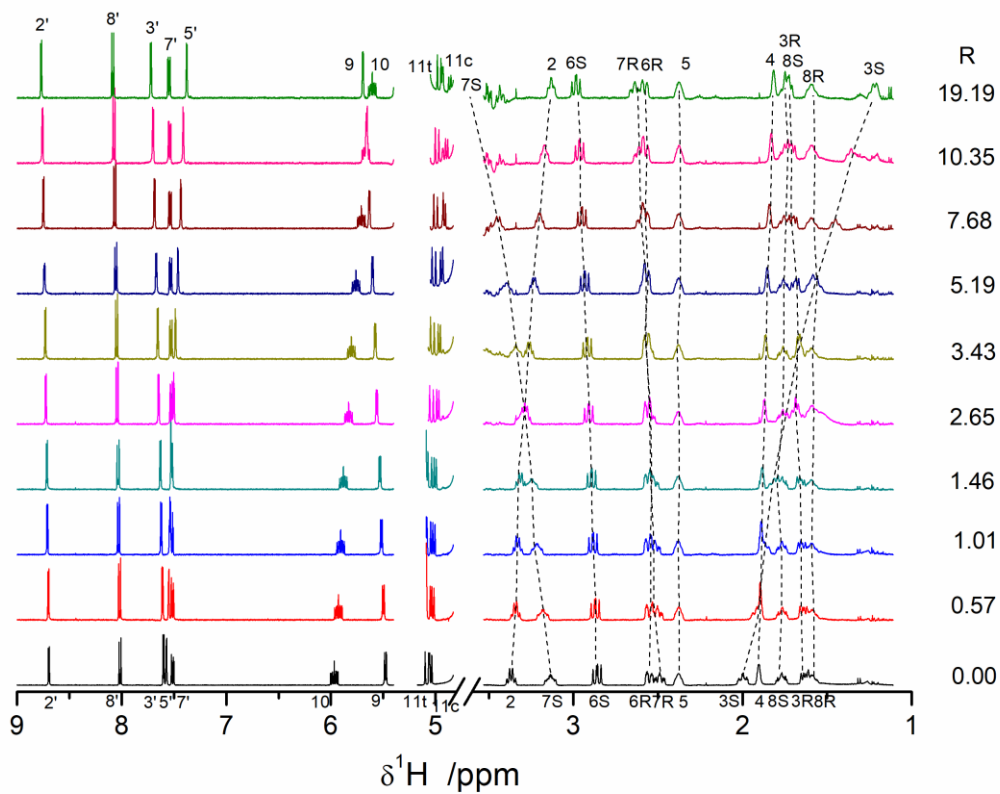


**Table S3**

Values of association constants,  $K_a$ , determined for quinine complexes with cyclodextrins at pH 10.5 (part A), pH 7.3 (part B) and 25°C. ND –  $K_a$  not determined since chemical shift changes were very small and scattered; X – hidden under H1 signal of  $\gamma$ CD.

Part A	K/ $\alpha$ CD	dK/ $\alpha$ CD	K/ $\beta$ CD	dK/ $\beta$ CD	K/ $\gamma$ CD	dK/ $\gamma$ CD
Quinoline moiety						
H2'	489	44	1641	152	368	25
H3'	374	9	1619	121	354	17
H5'	330	88	1378	92	334	12
H7'	ND		ND		370	53
H8'	180	82	1541	318	357	28
Me	489	44	2516	456	346	48
Linker						
H9	946	107	1608	122	352	14
Quinuclidine moiety						
H2	417	18	1524	118	349	13
H3R	265	17	1364	142	160	69
H3S	357	11	1296	141	363	51
H4	358	24	1263	119	360	38
H5	357	10	1222	53	ND	
H6R	410	17	417	150	795	361
H6S	1644	551	1596	109	381	23
H7R	366	8	1691	243	333	49
H7S	427	17	1715	174	505	90
H8R	514	32	1870	251	ND	
H8S	435	16	1548	124	55	45
H10	401	25	1442	89	341	11
H11c	391	15	1406	70	345	20
H11t	541	67	248	43	335	17
Part B						
Part B	K/ $\alpha$ CD	dK/ $\beta$ CD	K/ $\gamma$ D	dK/ $\beta$ CD	K/ $\gamma$ CD	dK/ $\gamma$ CD
Quinoline moiety						
H2'	ND		62	46	ND	
H3'	34	4	62	17	9	24
H5'	ND		152	80	ND	
H7'	ND		ND		ND	
H8'	ND		80	360	ND	
Me	ND		145	71	ND	
Linker						
H9	ND		257	308	38	27
Quinuclidine moiety						
H2	ND		ND		ND	
H3R	17	6	320	457	14	11
H3S	25	7	41	126	16	12
H4	ND		179	21	27	28
H5	35	8	136	18	ND	
H6R	14	6	116	20	ND	
H6S	55	11	128	37	ND	
H7R	33	2	208	61	ND	
H7S	ND		ND		ND	
H8R	ND		226	50	ND	
H8S	ND		344	35	30	60
H10	10	6	273	283	42	24
H11c	29	3	ND		X	
H11t	11	8	ND		X	

**Table S4**

$CIS(^1H)$  values, their standard deviations,  $\delta CIS(^1H)$ , and  $CIS(^{13}C)$  values determined for quinine complexes with cyclodextrins at pH 10.5 and 25°C.  $\delta CIS(^{13}C)$  are uniform and equal to 0.01 ppm.  $CIS(^1H)$  values were taken from a global analysis for those signals which were analyzed collectively.  $CIS(^1H)$  values for the remaining  $^1H$  nuclei (*italic*) and  $CIS(^{13}C)$  were calculated assuming fixed values of association constants  $K_a$  determined in the global analyses. All values are reported in ppm units. X - C2 quinine resonance was obscured by C6 of  $\alpha CD$  precluding determination of  $CIS(^{13}C)$ .

$^1H$	Q/ $\alpha CD$		Q/ $\beta CD$		Q/ $\gamma CD$		Q/ $\alpha CD$	Q/ $\beta CD$	Q/ $\gamma CD$	$^{13}C$
	$CIS(^1H)$	$\delta CIS$	$CIS(^1H)$	$\delta CIS$	$CIS(^1H)$	$\delta CIS$	$CIS(^{13}C)$			
Quinoline moiety										
H2'	0.043	0.001	0.104	0.003	0.096	0.002	0.34	0.26	-0.44	C2'
H3'	0.193	0.001	0.179	0.003	0.156	0.002	-0.59	-1.39	-1.80	C3'
H5'	-0.033	0.001	-0.158	0.003	-0.252	0.003	-0.45	-0.95	-1.36	C5'
H7'	<i>0.008</i>	<i>0.001</i>	<i>0.006</i>	<i>0.001</i>	0.046	0.002	0.10	-0.11	0.63	C7'
H8'	0.016	0.001	0.019	0.003	0.090	0.002	0.13	0.22	0.26	C8'
Me	<i>0.019</i>	<i>0.001</i>	<i>0.020</i>	<i>0.001</i>	<i>0.055</i>	<i>0.003</i>	-0.04	0.16	-0.01	Me
Linker										
H9	0.192	0.001	0.247	0.003	0.280	0.003	-2.18	-2.45	-1.13	C9
Quinuclidine moiety										
H2	-0.096	0.001	-0.186	0.003	-0.306	0.003	X	0.67	-1.64	C2
H3R	0.273	0.002	0.359	0.003	<i>0.124</i>	<i>0.009</i>	-0.37	-2.37	-5.00	C3
H3S	0.106	0.001	-0.289	0.003	-0.995	0.005				
H4	0.183	0.001	-0.145	0.003	-0.111	0.002	0.77	1.60	-0.06	C4
H5	0.134	0.001	-0.134	0.003	<i>-0.001</i>	<i>0.002</i>	2.19	2.42	-0.14	C5
H6R	<i>0.031</i>	<i>0.003</i>	<i>-0.016</i>	<i>0.001</i>	<i>0.037</i>	<i>0.003</i>	1.88	2.13	0.99	C6
H6S	0.272	0.002	0.365	0.003	0.161	0.002				
H7R	0.122	0.001	0.163	0.003	0.192	0.002	0.27	1.16	1.50	C7
H7S	0.102	0.001	0.402	0.003	<i>0.568</i>	<i>0.009</i>				
H8R	0.117	0.001	0.070	0.003	<i>-0.000</i>	<i>0.004</i>	0.16	1.36	0.00	C8
H8S	0.157	0.001	0.318	0.003	<i>-0.039</i>	<i>0.004</i>				
H10	0.109	0.001	-0.225	0.003	-0.471	0.003	-0.37	-0.87	-1.15	C10
H11c	0.044	0.001	-0.122	0.003	-0.238	0.003	1.40	1.70	0.20	C11
H11t	<i>0.015</i>	<i>0.001</i>	<i>-0.035</i>	<i>0.006</i>	-0.150	0.002				

**Table S5**

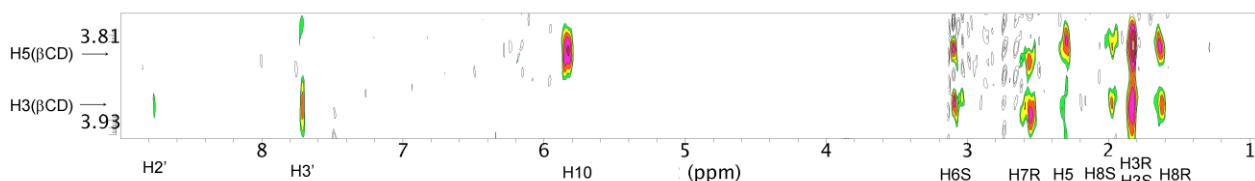
$CIS(^1H)$  values and their standard deviations,  $\delta CIS(^1H)$  – part A.  $CIS(^{13}C)$  values and  $\delta CIS(^{13}C)$  – part B. The reported data for quinine complexes with cyclodextrins were determined at pH 7.3 and 25°C.  $CIS(^1H)$  values were taken from a global analysis for those signals which were analyzed collectively. The  $CIS(^1H)$  values for the remaining  $^1H$  nuclei (*italic*) and  $CIS(^{13}C)$  were calculated assuming fixed values of association constants  $K_a$  determined in the global analyses. All values are reported in ppm units. ND - not determined due to the lack of complexation shift; X1 – H7S signal obscured by H3 of  $\alpha$ CD or  $\beta$ CD; X2 – quinine signals obscured by H1 of  $\gamma$ CD; X3 - C2 quinine signal obscured by C6 of the corresponding cyclodextrin.

Part A	Q/ $\alpha$ CD		Q/ $\beta$ CD		Q/ $\gamma$ CD	
	<i>CIS</i>	$\delta(CIS)$	<i>CIS</i>	$\delta(CIS)$	<i>CIS</i>	$\delta(CIS)$
Quinoline moiety						
H2'	ND		<i>0.040</i>	<i>0.003</i>	ND	
H3'	0.119	0.012	<i>0.065</i>	<i>0.003</i>	<i>0.190</i>	<i>0.010</i>
H5'	<i>0.061</i>	<i>0.006</i>	-0.022	0.005	ND	
H7'	<i>-0.021</i>	<i>0.003</i>	<i>-0.007</i>	<i>0.003</i>	ND	
H8'	<i>0.034</i>	<i>0.003</i>	<i>0.007</i>	<i>0.003</i>	ND	
Me	<i>0.029</i>	<i>0.004</i>	0.013	0.005	ND	
Linker						
H9	<i>-0.049</i>	<i>0.003</i>	<i>-0.059</i>	<i>0.010</i>	0.267	0.048
Quinuclidine moiety						
H2	<i>-0.131</i>	<i>0.041</i>	<i>-0.124</i>	<i>0.066</i>	<i>-0.248</i>	<i>0.025</i>
H3R	0.228	0.022	<i>0.021</i>	<i>0.005</i>	-0.531	0.092
H3S	0.203	0.020	<i>-0.095</i>	<i>0.016</i>	-1.415	0.242
H4	ND		-0.201	0.010	-0.201	0.038
H5	-0.119	0.012	-0.272	0.012	-0.334	0.041
H6R	-0.471	0.044	-0.304	0.013	<i>0.121</i>	<i>0.031</i>
H6S	<i>0.063</i>	<i>0.008</i>	-0.107	0.007	-0.334	0.059
H7R	-0.180	0.018	-0.239	0.011	<i>-0.087</i>	<i>0.027</i>
H7S	X1		X1		<i>0.296</i>	<i>0.054</i>
H8R	<i>-0.033</i>	<i>0.009</i>	-0.117	0.007	-0.180	0.035
H8S	<i>0.100</i>	<i>0.007</i>	<i>0.040</i>	<i>0.003</i>	-0.173	0.033
H10	0.203	0.020	<i>-0.044</i>	<i>0.007</i>	-0.243	0.044
H11c	0.145	0.014	<i>-0.064</i>	<i>0.011</i>	X2	
H11t	0.081	0.009	<i>-0.015</i>	<i>0.005</i>	X2	

Part B	Q/ $\alpha$ CD		Q/ $\beta$ CD		Q/ $\gamma$ CD	
	<i>CIS</i>	$\delta(CIS)$	<i>CIS</i>	$\delta(CIS)$	<i>CIS</i>	$\delta(CIS)$
Quinoline moiety						
C2'	0.13	0.01	0.00	0.01	-1.44	0.15
C3'	-0.04	0.01	-0.55	0.01	-2.32	0.24
C5'	0.08	0.01	-0.55	0.01	-3.15	0.32
C7'	-0.96	0.05	-0.28	0.01	0.22	0.02
C8'	-0.50	0.03	-0.26	0.01	-1.44	0.15
Me	-0.04	0.01	0.00	0.01	-0.61	0.06
Linker						
C9	-0.38	0.02	0.26	0.01	-0.64	0.07
Quinuclidine moiety						
C2	X3		X3		X3	
C3	1.67	0.09	0.81	0.02	-0.62	0.06
C4	2.26	0.12	1.64	0.03	0.22	0.02
C5	3.18	0.17	1.90	0.04	0.19	0.02
C6	2.43	0.13	1.49	0.03	-1.04	0.11
C7	-0.95	0.05	0.01	0.01	0.22	0.02
C8	1.84	0.10	0.00	0.01	1.02	0.11
C10	1.51	0.08	0.00	0.01	0.21	0.02
C11	1.42	0.07	0.00	0.01	-2.59	0.27

**Figure S6**

Stripe of 2D ROESY spectrum for Q/ $\beta$ CD complex. Area disturbed by cyclodextrin resonances (3.2 – 5.8 ppm on abscissa) was left blank for the clarity of presentation. Position of quinine and  $\beta$ CD resonances are marked on the abscissa and ordinate, respectively.

**Table S6**

The 23 DFT derived lowest-energy conformations. Energies,  $E$ , are given in kcal/mol, molecular dipole moments,  $\mu$ , in debyes, scalar coupling constants,  $J$ , in hertz, and  $\phi_1 - \phi_5$  corresponding to dihedral angles  $H_2-C_2-C_9-H_9$ ,  $H_9-C_9-C_4-C_3'$ ,  $H_5-C_5-C_{10}-H_{10}$ ,  $C_5-C_6-O-C_{Me}$ , and  $H-O-C_9-H_9$ , in degrees. Definitions of the dihedral angles are given in Figure S2.

Struct.	$E$	$\mu$	$J_{2,9}$	$J_{5,10}$	$\phi_1$	$\phi_2$	$\phi_3$	$\phi_4$	$\phi_5$
C1	0.00	6.57	7.49	8.73	39.5	-141.1	-177.1	-0.9	-136.0
C2	0.07	4.32	1.31	8.55	-74.9	-142.5	-177.4	-0.1	53.0
C3	0.32	5.58	8.56	8.58	178.5	10.0	-176.7	0.1	55.2
C4	0.65	6.09	1.31	8.55	-74.9	-142.5	-177.5	-0.1	53.0
C5	0.65	6.09	8.03	8.62	178.1	-173.2	-176.9	-0.7	57.3
C6	0.87	5.33	1.50	8.52	-74.8	-138.9	-177.3	-0.1	-165.9
C7	0.87	5.33	8.69	8.46	177.0	144.8	-177.8	0.3	175.0
C8	1.01	7.00	7.60	3.71	39.0	-141.1	62.9	-0.9	-135.9
C9	1.08	7.89	8.28	8.60	-178.9	11.5	-176.6	0.1	-54.6
C10	1.16	5.57	7.50	8.72	39.6	-140.5	-176.9	-179.9	-136.0
C11	1.27	8.17	7.79	8.63	-179.4	-173.3	-176.6	-0.9	-56.4
C12	1.29	2.36	1.31	8.55	-75.0	-142.0	-177.2	179.9	52.5
C13	1.33	6.91	7.39	2.76	39.9	-141.6	-76.7	-1.0	-137.3
C14	1.33	4.49	1.36	3.81	-74.5	-142.7	61.7	-0.2	53.1
C15	1.35	5.22	1.50	8.53	-74.8	-138.9	-177.4	-0.2	-165.8
C16	1.47	6.71	0.94	8.43	-77.6	-140.5	-178.3	-0.1	-42.4
C17	1.56	8.04	8.31	8.56	179.0	142.2	-177.1	0.3	-48.3
C18	1.57	5.99	8.65	3.77	178.4	10.1	62.2	0.4	55.0
C19	1.60	2.16	8.53	8.56	178.0	8.7	-176.7	179.6	54.9
C20	1.73	4.65	1.36	2.99	-74.3	-142.7	-73.5	-0.4	52.5
C21	1.78	4.58	8.03	8.63	179.3	-170.1	-176.6	-180.0	57.6
C22	1.85	6.46	8.15	3.84	178.7	-172.2	61.5	-0.8	57.6
C23	1.96	4.77	8.58	3.02	178.1	9.5	-73.1	0.0	55.1

### Figure S7

Histogram of dipole moment values displays a gap between three conformers with the largest  $\mu$  value (C9, C11, and C22 in Table S4) and the rest of them.

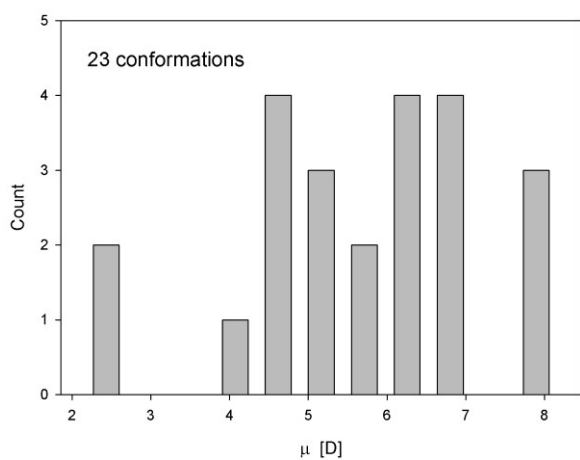
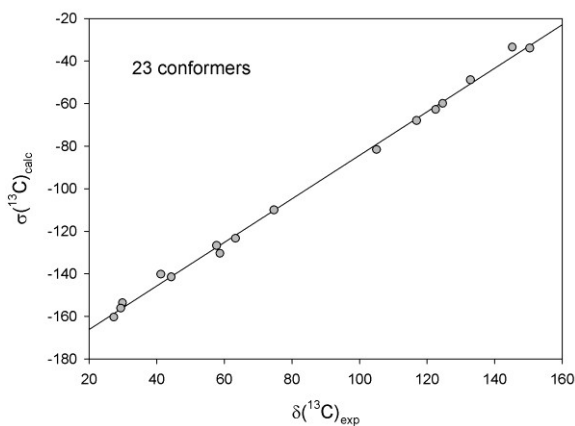
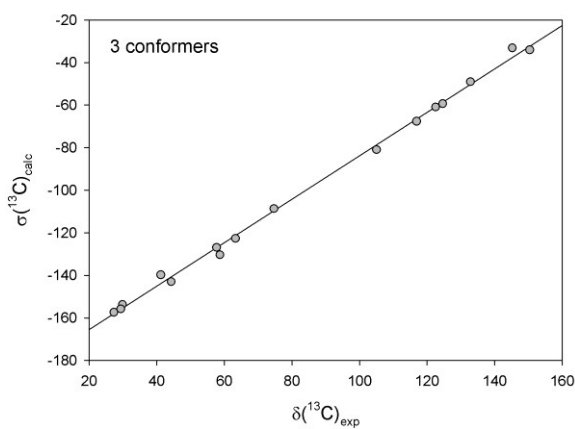


### Figure S8

Correlations between DFT derived  $^{13}\text{C}$  shielding constants population averaged for the group of 23 lowest-energy conformers using Boltzmann factors and experimental chemical shifts for the proton bearing  $^{13}\text{C}$  nuclei of quinine in aqueous solution at pH 10.5. Standard errors of estimates were 2.38 ppm and 2.40 ppm for 3 and 23 conformers, respectively.



## DFT based parametrization of Karplus equation for vicinal ${}^3J_{2,9}$ coupling constant in neutral quinine molecule in aqueous solution

In order to fulfill calibration requirement in a particular case of quinine molecule, theoretical values of  ${}^3J_{2,9}$  coupling constant between protons H2 and H9 were calculated by the DFT method at fixed values of H<sub>2</sub>–C<sub>2</sub>–C<sub>9</sub>–H<sub>9</sub> dihedral angle  $\phi_1$ . It was set to the multiplicities of 30 deg while all other degrees of conformational freedom were optimized. The Karplus curve based on these calculations is shown in the Figure S5.

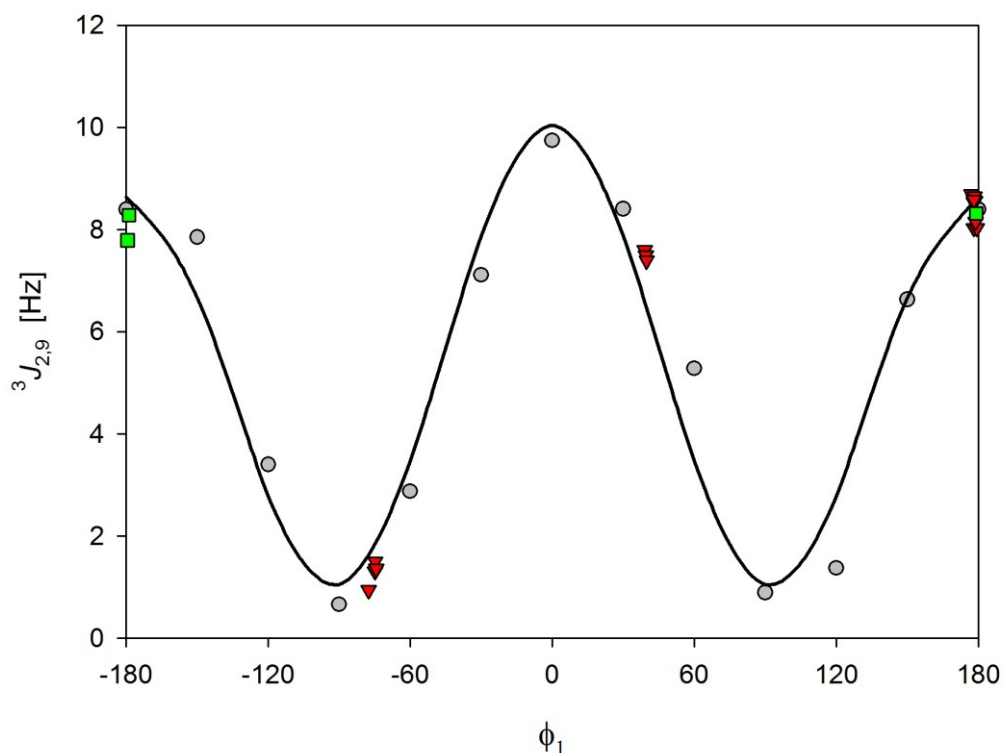


**Figure S9**

Solid line corresponds to the best fit of Karplus equation:  ${}^3J(\theta) = A \cos 2\theta + B \cos \theta + C$ , to the DFT derived data represented by gray circles. Equation parameters and their standard errors (in parentheses) are as follows:  $A = 4.14$  (0.36) Hz,  $B = 0.70$  (0.36) Hz,  $C = 5.19$  (0.26) Hz. Green squares represent three conformations with the largest dipole moments which prevail in aqueous solution of quinine. The remaining of the 23 lowest-energy conformers are shown as red triangles.

## Influence of Q/CD complex formation on values of vicinal ${}^3J_{5,10}$ coupling constant

The values of  ${}^3J_{5,10}$  coupling constant in quinine have been measured in all titration experiments. The data obtained at pH 10.5 are shown in the Figure S7. With the aid of already determined association constants the  ${}^3J_{5,10}$  values have been extrapolated to the complexed forms and the results are given in the Table S5. The value observed in Q/ $\beta$ CD complex is higher than that in the non complexed quinine. It means that the space available for the quinolidine part inside the  $\beta$ CD cavity is limited and conformers with large  $\phi_3$  value are only allowed. This effect is also observed in the case of Q/ $\alpha$ CD complex but is somewhat smaller

since the quinolidine moiety penetrates less deeply into the  $\alpha$ CD cavity. In the case of  $\gamma$ CD there is enough space inside the CD cavity to retain the conformational equilibrium on C5–C10 bond. Therefore,  $^3J_{5,10}$  coupling constant does not change its value. Again, the observed changes reflect well the bimodal mode of binding.

**Figure S10**

$^3J_{5,10}$  coupling constants obtained from titration data and the best fit curves for Q/CD complexes at pH 10.5.  $R$  - ratio of host to guest molar concentrations.

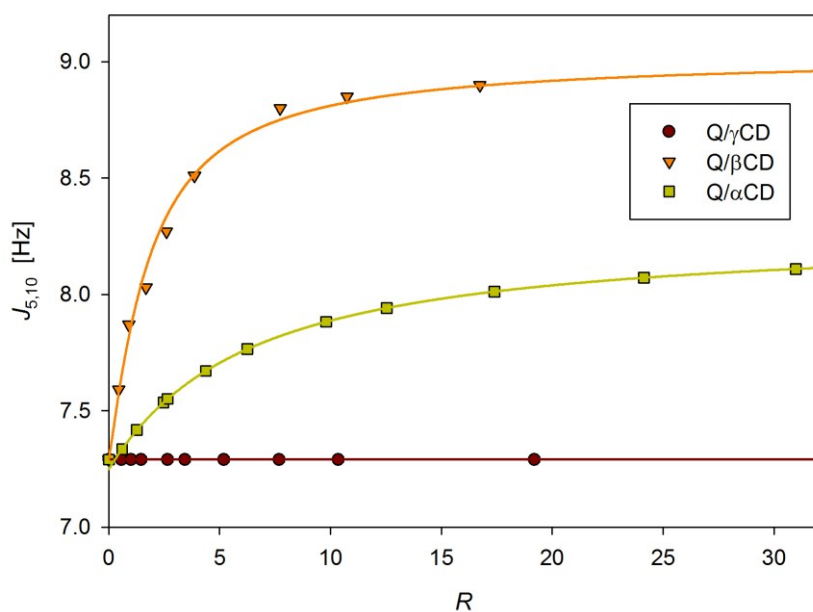


**Table S7**

$^3J_{5,10}$  coupling constant measured in  $D_2O$  at pH 10.5 (isotope uncorrected) for quinine and obtained from titration data for its inclusion complexes with cyclodextrins. All values are given in hertz, accuracy ca. 0.1 Hz, temperature 25°C.

$^3J_{5,10}$	Q	Q/ $\alpha$ CD	Q/ $\beta$ CD	Q/ $\gamma$ CD
	7.3	8.3	9.0	7.3